


Mechanism of Cu^{2+} and reactive yellow 145 dye adsorption onto eggshell waste as low-cost adsorbent

[Edwin A. Ofudje](#) , [Ezekiel F. Sodiya](#), [Francis H. Ibadin](#), [Abimbola A. Ogundiran](#), [Samson O. Alayande](#)  & [Oluremi A. Osideko](#)

Received 06 Apr 2020, Accepted 18 Nov 2020, Published online: 26 Dec 2020

Chemistry and Ecology

Taylor & Francis, Vol 36, issue 10. Page 1-22

ABSTRACT

This work presents low-cost sorbent powder obtained from agro-waste of poultry eggshells for the adsorption of contaminants and was elucidated with transmission electron microscopy, Fourier transform infrared, scanning electron microscope, X-ray diffraction and N_2 adsorption–desorption techniques. It was observed that a solution pH of 2.0 and 5.0 was enough for the maximum uptake of reactive yellow 145 dye (RY 145) and $\text{Cu}(\text{II})$ ions, respectively, which showed that the pollutants removal was affected by the pH of solution. Langmuir monolayer adsorption capacity was found to be 101.500 mg/g for $\text{Cu}(\text{II})$ and 88.450 mg/g for reactive yellow 145 dye, respectively. Redlich–Peterson and Sips models both fitted well with the adsorption data. The Pseudo-second-order equation demonstrated good relationship with the experimental data and thus explained the adsorption mechanism to be chemisorption. Values of different thermodynamic considerations gave the values of ΔH° and ΔS° to be 30452.020, 27194.180 and 100.930, 90.370 kJmol^{-1} for $\text{Cu}(\text{II})$ and RY 145 dye, respectively. Findings from this current study revealed that the prepared sorbent from agro-waste of eggshell can be a useful material for the elimination of $\text{Cu}(\text{II})$ and RY 145 dye in aqueous solutions.

KEYWORDS:

[Adsorption equilibrium kinetics mechanism reactive yellow 145](#)

Introduction

Human activities caused by contaminants like heavy metals, dyes, insect repellent and herbicides have negatively impacted the health and economic condition of the populace. An increase in populace and agricultural practices coupled with advancement in industrialisation and lack of proper implementations of environmental regulations had worsened the circumstances [1]. Since heavy metals are stable to degradation, they can, therefore, set down in the water and could bioaccumulate through food chain and results in individual health danger [2,3]. Some of the causes of these metals include industrialised actions such as painting, dyeing, electroplating, mining,

agricultural practices like pesticides, herbicides and fertiliser applications and household actions which result in the release of pollutants into the water system [4,5]. Copper which is an important constituent of living organisms occurs in metalloproteins like haemocyanin which carries oxygen in plastocyanin and cytochrome oxidases, arthropods and molluscs [6]. Ailments such as liver and kidney damage, anaemia, stomach and intestinal irritation may be caused by the high ingestion of copper doses [7]. Reactive dyes are extensively utilised as dyeing agent in the textile industry because they are anionic compounds which are soluble in water as a result of the existence of a sulfonic group in the molecule which enables them to fix covalently to the textile fibres macromolecules [8]. Besides causing low aesthetics in freshwater, toxic derivatives of dyes produced through hydrolysis, oxidation and/or other (bio) chemical reactions can as a well-posed danger to the environment [8].

Several processes among which includes precipitation, membrane filtration, ion-exchange, flocculation, ozonation or oxidation, photocatalytic degradation, electrochemical degradation and adsorption had been used for the decontamination of polluted water [9–11]. Among these techniques, adsorption is widely used due to less capital investment, ease to design and operate and eco-friendly [12]. Commercially activated carbon is widely used as an effective adsorbent in the adsorption process; however, high cost of production often limits its applications. Thus, there is a need to seek for cheap and eco-friendly materials that can serve as alternative adsorbents to the conventional activated carbon. To this end, some adsorbents such as fish scale [5], biochar [13], fungal strain isolate [14], chitosan–carboxymethyl starch composites [15], *Spinacia oleracea* [16], ostrich eggshell [17], coconut shaft [18] and guinea corn [19] had been effectively utilised in the elimination of pollutants from contaminated water.

Eggshells are sources of environmental pollution not only in poultry farming but also in the society at large since they are present in large volumes. Discarded eggshells could be a source of diseases because the high content of organic matter could harbour bacteria and fungi coupled with the horrible smell it generates [17]. In this study, the waste generated from eggshell powder was utilised as a cheap adsorbent for the elimination of copper ions and reactive yellow 145 dye from aqueous solution via batch adsorption process under diverse experimental operations. Fourier transform infrared (FT-IR), X-ray diffraction (XRD), transmission electron microscopy (TEM) and scanning electron microscope (SEM) studies were deployed to elucidate the composition of the adsorbent. Different isotherms and kinetic models were deployed to evaluate the adsorption equilibrium and kinetic data. Thermodynamic operations were evaluated to assess the role of temperature on the sorption process.

Materials and methods

Chemicals

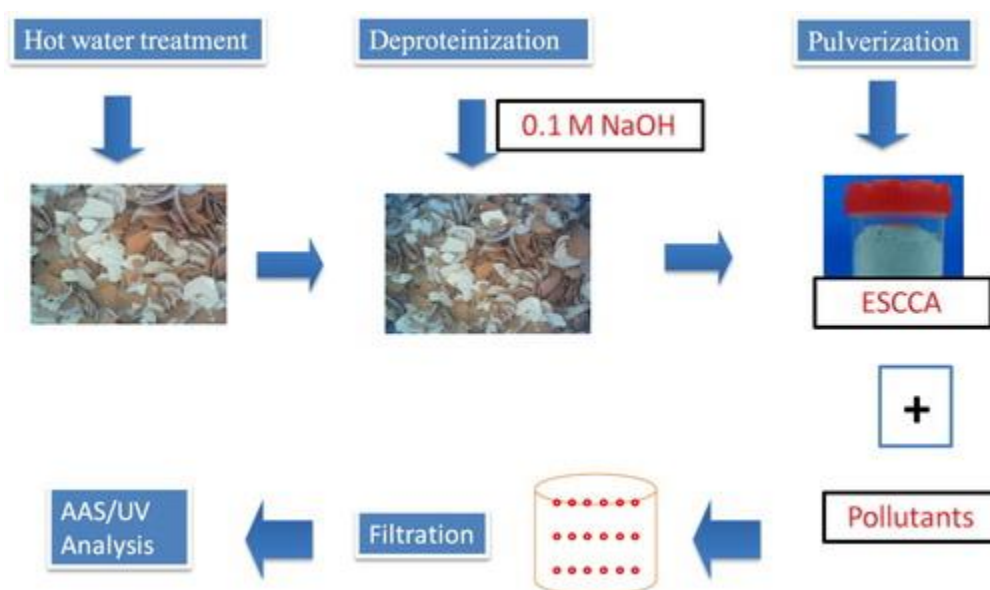
All commercial chemicals used were of analytical grade. Copper stock solution (1000 mg L^{-1}) was prepared by dissolving 99.999% purity elemental copper (Sigma-Aldrich) in nitric acid and diluting with ultra-pure water. The Reactive yellow 145 dye was utilised as adsorbate in this study has a molecular formula (MF: $\text{C}_{28}\text{H}_{20}\text{ClN}_9\text{Na}_4\text{O}_{16}\text{S}_5$) with a molecular weight of 1026.26 g/mol and λ_{max} in an aqueous solution of 416 nm . For the dye, a stock solution of 1000 mg L^{-1} was made by dissolving 1.00 g of dye in 1 L distilled water. Several ranges of concentrations of the pollutants

(10–150 mgL⁻¹) were made from these stock solutions by serial dilutions. Adjustment of solution pH was achieved by adding either 0.1 M HCl or NaOH solutions.

Preparation of adsorbent

Waste eggshells were sourced locally from a poultry farm and cleaned with hot water to get rid of any unnecessary material which stocked on its surface. Samples were thereafter boiled with 0.1 M of NaOH to remove organic matter, rinsed with distilled water and then oven-dried at 100°C for 12 h and reduced to small pieces by pulverisation. The products obtained were filtered to get the desired particle size and labelled as eggshell derived calcium carbonate adsorbent (ESCCA). The schematic representation of the processing of the eggshell for the sorption of contaminants is shown in [Figure 1](#).

Figure 1. Schematic representation of adsorbent preparation and adsorption process.



[Display full size](#)

Characterisation of adsorbent

Nanotracer which is equipped with Microtrac FLEX 10.5.2 was used for particle size analysis in which samples (about 0.1 g) were dispersed in 50 mL of Millipore water in 100 mL beaker and sonicated for 10 min to minimise the degree of agglomeration of the particle. The zeta potential of the adsorbent was evaluated using a Zetasizer Nano ZS instrument (Malvern, UK). Functional group determination was obtained using FT-IR spectroscopy (model 8400S (Shimadzu, Japan)). A ratio of 1:99% of the adsorbent powder and KBr were mixed with the aids of mortar and pestle and thereafter compressed to form pellet of 2 mm at about a load of 5 tons. The FT-IR spectrums were measured within the range of 400 cm⁻¹–4000 cm⁻¹ at a resolution of 4 and 64 times scanning. The phase characterisation was done by XRD using PANalytical (X'Pert Pro, Netherlands). Diffraction electrons were obtained over a range of $2\theta = 10^\circ$ – 60° with an incremental step size of

0.02 using Cu K α ($\gamma = 1.54178 \text{ \AA}$) radiation. SEM and TEM analyses were done to evaluate the morphology as well as the elemental composition of the sorbent with the aid of Hitachi (Japan) S-3000H electron microscope with an accelerating voltage of 15 kV equipped with EDX and TEM (Tecnai 20 G2 FEI, Netherlands), respectively. Particles of ESCCA were dispersed in distilled water and sonicated for 10 min and a drop was made on a copper grid.

Batch adsorption study

Different concentrations (10–150 mg/L) of Cu(II) ions and RY4 dye were placed in a series of separate 100 mL beakers. A 25 mg of the prepared sorbent was introduced into the respective flask and left to agitate for specific contact time (5–120 min) on orbital shaker at a speed of 150 rpm and temperature of ($35^\circ\text{C} \pm 1^\circ\text{C}$). Adjustment of the solution pH was done using 0.1 M NaOH or HCl in the range of pH 2–10. After attaining equilibrium, the flask content was centrifuged at a speed of 2500 rpm for 10 min and the concentrations of the Cu(II) ions and RY145 dye in the filtrate were estimated using Atomic Absorption Spectrophotometer and UV–VIS spectrophotometer, respectively. The amounts adsorbed as well as the removal percentage of pollutants were computed using the following equations, respectively: $Q_e = C_o - C_e m \times V$

$$(1) \% \text{Removal} = \frac{C_o - C_e}{C_o} \times 100$$

(2)

Q_e stands for the amount of pollutants adsorbed in mg/g, C_o and C_e are the initial and equilibrium concentrations of pollutants in mg/L, respectively, ‘ m ’ represents the mass of the sorbent and ‘ V ’ is the volume of the adsorbate used in litre.

The adsorption mechanisms of the pollutants onto ESCCA were achieved with Elovich, Pseudo-first-order, Pseudo-second-order and intra-particle kinetic diffusion models [20–22] as described in Equations (3)–(6): $q_t = 1/\beta (\ln \alpha \beta) + (1/\beta) \ln t$

$$(3) Q_t = Q_e (1 - e^{-k_1 t}) \quad (4) Q_t = k_2 Q_e t / (1 + k_2 Q_e t) \quad (5) Q_t = K_{id} t^{0.5} + C_i$$

(6)

The Pseudo-first- and second-order kinetic models rate constants are given as k_1 (min^{-1}) and k_2 ($\text{min}^{-1} \text{g/mg}$) respectively. Whereas, the Elovich rates of adsorption and desorption are given as α and β in mg/g/min and gmg^{-1} respectively. K_{id} stands for the intra-particle diffusion rate constant in $\text{mgg}^{-1} \text{min}^{-0.5}$ and C_i is the intercept and a measure of the surface thickness of the adsorbent. The plots of Q_e against t using Scientist software were used to estimate all the constants.

Test of kinetic fitness

The comparison between the Pseudo-first- and second-order models were tested using the sum of error squares (SSE, %) [23]: $\%SSE = \frac{((Q_{(exp)} - Q_{(Calc)}) / Q_{exp})^2 N - 1}{\sqrt{\dots}} \times 100$

(7)

The data point's number is given as N .

To examine the sorption ability of the adsorbent, Freundlich, Temkin, Langmuir and Dubinin–Radushkevich (D–R) which are two-parameter isotherms were used in addition to three-parameter isotherms such as Redlich–Peterson (R-P) and Sips which are listed in Equations (8)–(13) [24–30]: $Q_e = Q_o b C_e^{1+b}$

$$(8) \quad Q_{eq} = K_F C_e^n \quad (9) \quad Q_e = RT b_T \ln a_T C_e \quad (10) \quad Q_e = Q_s \exp\left(-\frac{RT \ln(1 + C_e)}{2E}\right) \quad (11) \quad Q_e = Q_o C_e / (1 + K_R C_e) \quad (12)$$
$$Q_e = Q_s (K_s C_e)^{\beta} / (1 + (K_s C_e)^{\beta})$$

(13)

where Q_o (mg/g) and b (mg/L) are parameters of the Langmuir isotherm which stand for the maximum monolayer adsorption capacity and the energy of adsorption, respectively, K_F (mg/g)(mg/L) and n are the Freundlich isotherm's constants being the sorption capacity and adsorption strength of the sorbent. The values of a_T (L/g) and b_T (J/mol) of the Temkin constant relating to the binding energy and the heat of adsorption, respectively. From the D–R isotherm, Q_m represents the saturation sorption ability of the sorbent, while β stands for the free energy of adsorption and ϵ is the Polanyi potential, that can be expressed as: $\epsilon = RT \ln(1 + 1/C_e)$

, given that the ideal gas constant is represented as R (8.31 J/mol/K) and T is the temperature (K). The mean sorption energy values, (E) in kJ/mol, is known as the change in free energy that is needed to transfer 1 mol of adsorbate from solution to the surface of the adsorbent and can be estimated from the parameter β as follows: $E = 12\beta$

(14)

Information obtain from E (kJ/mol) could be used in predicting the mechanism of adsorption. For instance, values of E between 8 and 16 kJ/mol corresponds to ion-exchange process, while E values less than 8 kJ/mol signifies physical adsorption and when the value of E is higher than 16 kJ/mol, it denotes particle diffusion [27,30]. For the three-parameter isotherms, the Redlich–Peterson isotherm constant is given as K_R , (mg/L); g stands for the Redlich–Peterson isotherm exponent that ranges between 0 and 1. Both Langmuir and Freundlich isotherms can be successfully obtained from the R-P isotherm. If β is 1, the equation for R-P reduces to Langmuir isotherm equation; but it reduces to Freundlich isotherm equation for β equals 0 [28,29,31]. From the Sips isotherm, K_s is the equilibrium constant (mg/L), Q_s stands for the maximum Sips's sorption capacity (mg/g), the exponent (β_s) which when equals to 1, then the equation becomes Langmuir equation and reduces to Freundlich isotherm as either C_e or K_s tends towards 0 [28,29,31].

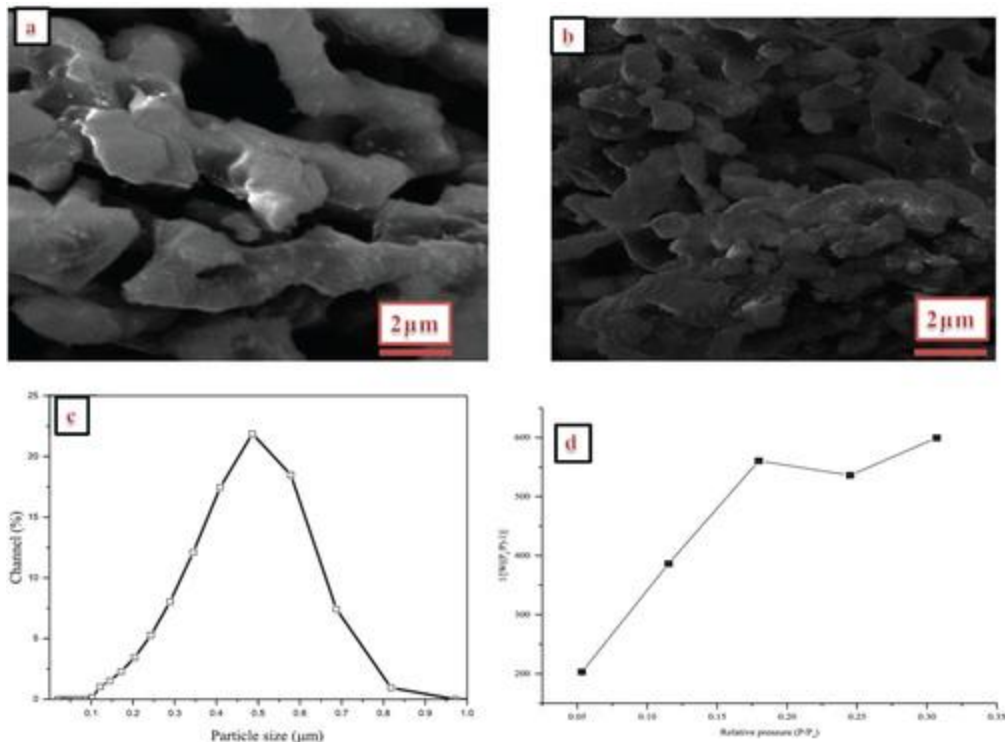
Results and discussions

Characterisations

Table 1 presents the physical parameters of the fabricated sorbent with the surface area, pore size, pore-volume and bulk density found to be (113.72 m²/g), (2.36 nm), (0.27 cm³/g), (1.27 cm³/g) and (1.26 g/cm³), respectively. SEM image (Figure 2(a,b)) of the eggshell before and after adsorption shows the morphological feature of the adsorbent surface as consisting of nearly round particles that agglomerated together after adsorption process. Open pores which were noticed on the surface of the eggshell before the uptake process was absent after the adsorption of the pollutants. The vacant sites available on the surface of the ESCCA were filled up by the diffused adsorbate particle. The particle size distribution (Figure 2(c)) of the ESCCA was found to be between 0.2 and 0.9 μm. Analysis of TEM (Figure 3(a)) shows that the structure of the eggshell particles is composed of round morphology with length and breadth of 98 and 34 nm, respectively. Information from selected area electron diffraction (SAED) revealed non-spotted and non-continuous rings thus suggesting large non-crystalline grains as depicted in Figure 3(b). FT-IR spectra (Figure 4(a)) of the adsorbent demonstrate vibration bands at 715, 875, 1457 and 2516 cm⁻¹ which are attributed to the main peaks of CaCO₃ [32,33]. Also, the bands noticed at around 1787, 2878 and 2987 cm⁻¹ were allotted to C=O of carbonate ion (CO₂₋₃

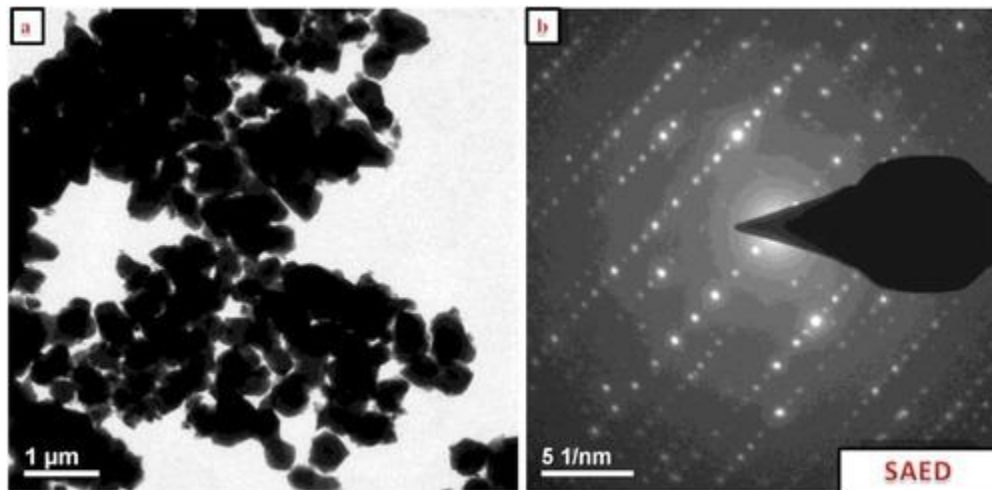
) [33]. The sharp peak observed at 1105 cm⁻¹ was assigned to C-O bonds of carbonate, while Ca-O bond was observed at around 587 cm⁻¹. The broad band which corresponds to the moisture absorption on the surface of the prepared adsorbent was observed at 3413 cm⁻¹ [32,33]. However, after the adsorption process, prominent absorption peaks initially observed at 1105, 1457, 1787 cm⁻¹, 2987cm⁻¹ and 3413 cm⁻¹ for the raw eggshell have shifted to 1112, 1466, 1792 cm⁻¹, 2989cm⁻¹ and 3450 cm⁻¹ after the adsorption of Cu(II) ions and 1107, 1460, 1784 cm⁻¹, 2979cm⁻¹ and 3568 cm⁻¹ after the uptake of RY 145 dye, respectively. These changes in the FT-IR results revealed that there are interactions between the functional groups of the eggshells with the positive charges of the pollutants, thus suggesting electrostatic adsorption mechanism. According to Bartczak et al. [34], heavy metals ions form bonds with oxygen groups present of the functional groups and that a slightly shifts in the maximal wavenumbers of the functional groups involved in creation of the interactions between hazardous metal ions and the surface of the adsorbent. It is apparent from the FT-IR spectra also that carbonyl and hydroxyl groups were the main adsorption sites present in abundance on the surface of the eggshell powder. These groups which could serve as proton donors; when deprotonated may be engaged in coordination with the positive charges on the surface of the pollutants.

Figure 2. (a) SEM analysis of raw eggshell, (b) SEM analysis of eggshell after adsorption, (c) particle size of eggshell and (d) BET N₂ adsorption isotherm analysis.



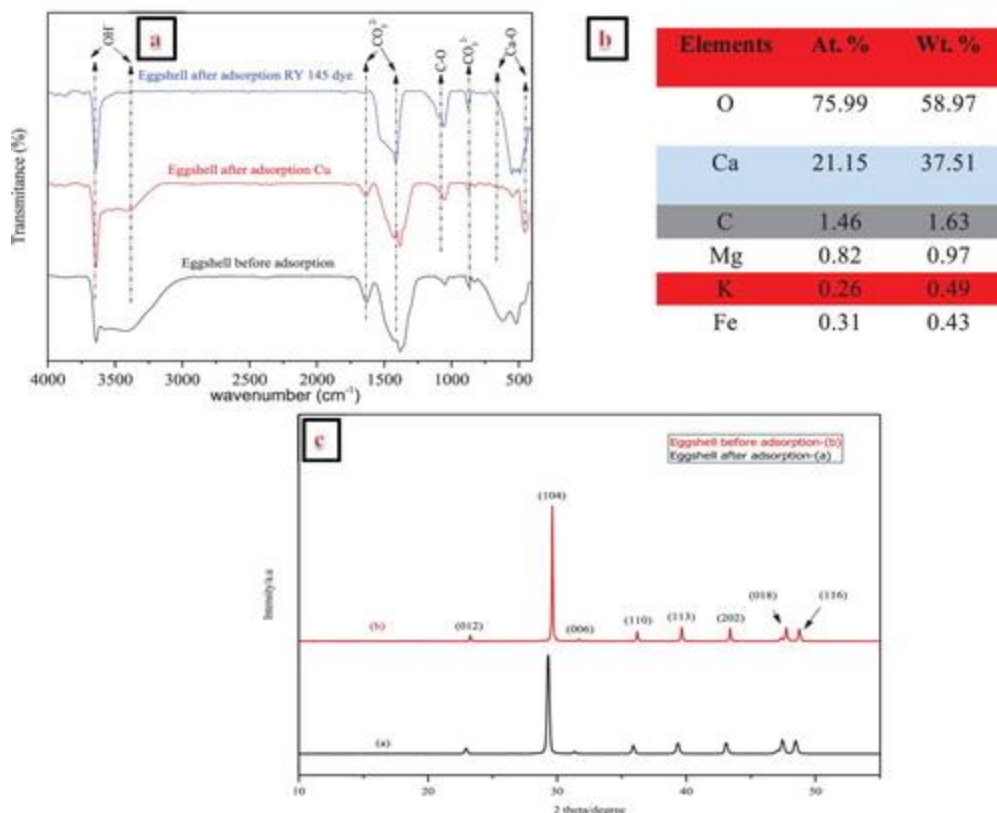
[Display full size](#)

Figure 3. (a) TEM analysis of eggshell and (b) SAED of eggshell.



[Display full size](#)

Figure 4. (a) FT-IR spectra of ESCCA before and after adsorption, (b) EDAX measurement of ESCCA and (c) XRD analysis of ESCCA before and after adsorption.



[Display full size](#)

Table 1. Physical parameters of chemically synthesized ESCCA.

[CSVDisplay Table](#)

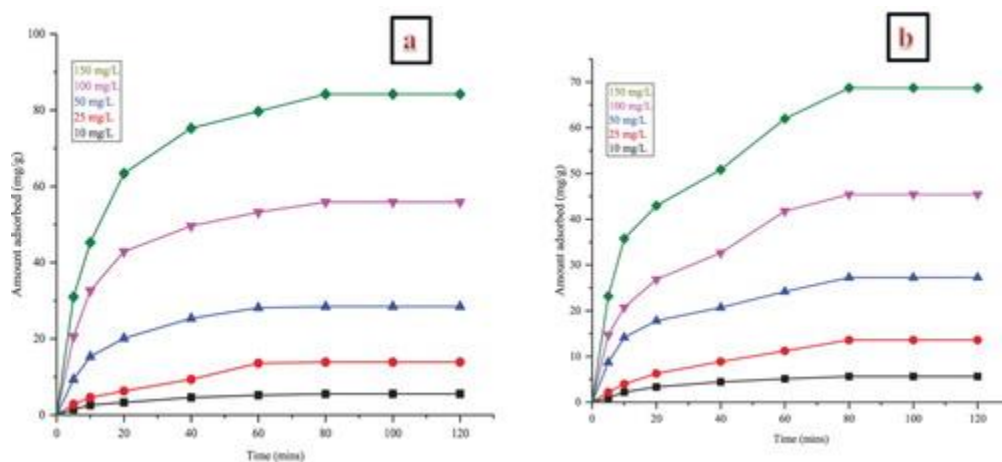
EDX spectrum ([Figure 4\(b\)](#)) shows the existence of elements such as K, Ca, Mg, Fe, C and O in the shell with carbon, calcium and oxygen having large proportions. The XRD pattern ([Figure 4\(c\)](#)) of the eggshell was compared with calcite data from JCPDS with file no. 47-1743 which matched well with standard data. This suggests that the crystalline phase present in the shell was calcite having Rhombohedral crystal structure [33]. Prominent planes such as (104), (012), (110), (113), (202), (018) and (116) corresponding to crystalline calcite were observed. After the adsorption process, a shift in peaks positions was observed; however, no new phase was present.

Effect of the initial concentration of contaminants and contact time

[Figure 5](#) presents the role of contact time on the pollutants uptake onto the surface of the as-prepared adsorbent at different initial pollutant concentrations. The results show that the amount of the pollutants sorbed rise with the agitation time and attained a constant value after which pollutants removal from the solution was no longer feasible. The adsorption process can be grouped into two steps: (1) a rapid adsorption occurring at the first 20 min which is due to the available vacant sites on the surface of the ESCCA; and (2) a slow adsorption process until the

equilibrium point was reached at 80 min of contact time and there was no further appreciable uptake of pollutant by the adsorbent. The sorbed adsorbate adhered to the free sites of the ESCCA surface as the reaction proceeds. The plots equally showed that pollutant adsorption increases with the concentration of the contaminants. Maximum adsorption of Cu(II) ions and RY 145 by ESCCA attained equilibrium at 80 min of contact time for initial pollutant concentration of 150 mg/L (84.20 mg/g) for Cu(II) ions (Figure 5(a)) and (68.70 mg/g) for RY 145 dye (Figure 5(b)), respectively. The results obtained by Kumar et al. [35] showed that the maximum uptake of Cu(II) ions from aqueous solution was effective at biomass dosage of 0.75 g in case of groundnut seed cake powder and 1.0 g when sesame seed cake and coconut seed cake powder were used. Li et al. [36] observed that greater pollutant concentration creates a better driving force to overcome the resistance from the mass transfer of adsorbate between the adsorbent and the aqueous phase which then enhanced the elimination of the adsorbate by the adsorbent.

Figure 5. Effect of contact time and initial pollutants concentration on the adsorption process of (a) Cu(II) and (b) RY 145 dye at solution pH of 2 and 5, biomass dosage of 25 mg and temperature of 45°C.

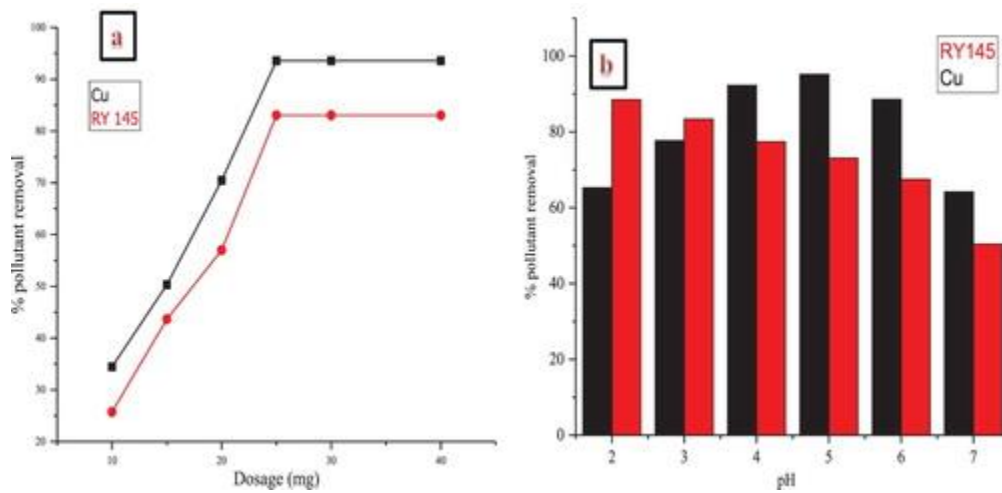


[Display full size](#)

Effects of dosage

The results presents in Figure 6(a) revealed a rapid removal of pollutants which rise with the adsorbent dosage until equilibrium was achieved. This is due to the availability of empty active spots on the adsorbent surface which enhances the number of pollutants adsorbed per unit time [23,37]. It was noticed that when the dosage of the adsorbent was adjusted from 10 to 25 mg, the percentage adsorption of Cu(II) rise from 34.43% to 93.56%, while that of RY 145 dye increased from 25.73% to 84.05%. Above this amount (25 mg), there was no appreciable rise in the removal efficiency of both Cu(II) and RY 145 dye and this is because of the saturation of the active vacant receptors on the adsorbent surface. This is similar to the report of Adeogun et al. [5] in which an increase in the adsorption capacity of tilapia fish scale biomass was observed with an increase in the adsorbent dosage and this was attributed to an increase in the adsorbent surface areas, augmenting the number of adsorption sites available for adsorption.

Figure 6. Effect of (a) adsorbent dosage and (b) solution pH on the adsorption process at a contact time: 80 min, initial pollutants concentration: 150 mg/L and temperature: 45°C.



[Display full size](#)

Effects of solution pH

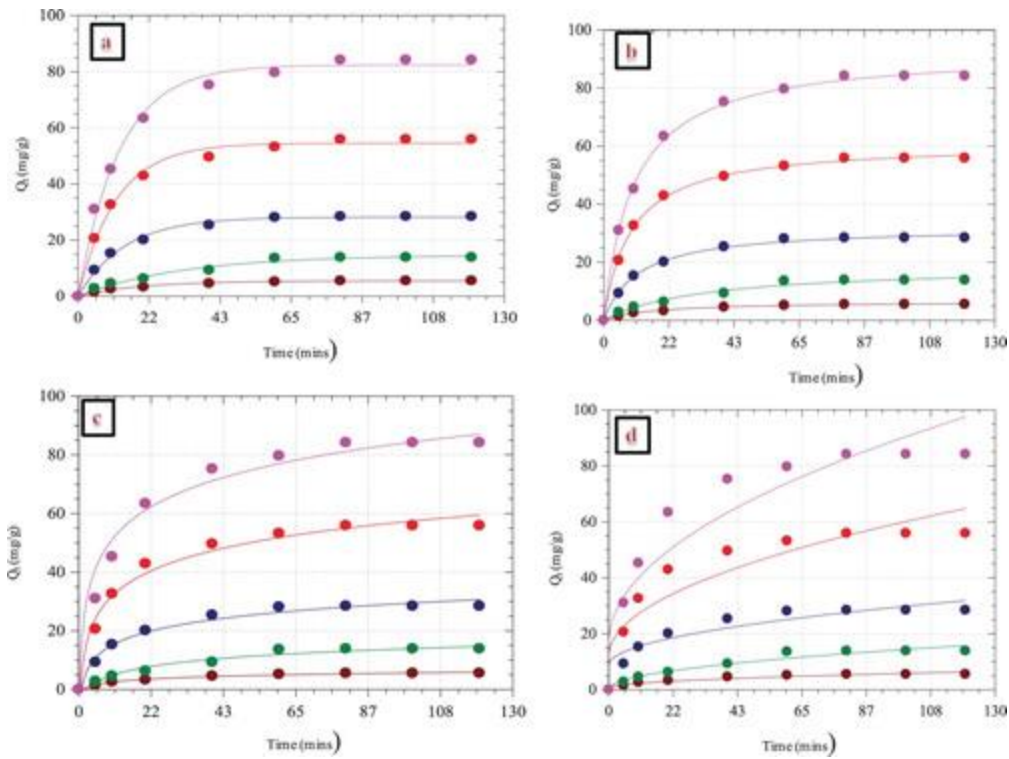
The adsorption of Cu(II) and RY 145 dye onto ESCCA at diverse pH range of 2.0–7.0 was conducted and the results is as depicted in [Figure 6\(b\)](#). It was noticed that while the percentage removal of Cu(II) ions rises with solution pH up to 5.0, that of the RY 145 dye decreases drastically. Maximum uptake of 95.20% and 88.50% was attained at a solution pH of 5.0 and 2.0 for Cu(II) ions and RY 145 dye, respectively. These actions can be viewed by observing the alterations in the ionic state of the various functional groups present on the adsorbent surface as revealed by FT-IR investigation and also those on the adsorbate solution (RY 145) and the charge of the Cu(II) at various pH values. Since RY 145 is an anionic dye, adsorbent surface with positive charges would be more important to its removal at lower pH value (acidic), while on the other hand, the negative form of ESCCA would be useful in the uptake of Cu(II) ions. In the case of the reactive yellow 145 dye, at lower solution pH, these functional groups are highly protonated, and as such the electrostatic attraction between ESCCA and RY 145 is very strong which enhanced the uptake of RY 145 dye. But when the solution pH increases, the functional groups are deprotonated, thus reducing the electrostatic attraction and as such the RY 145 dye can no longer bound effectively to the negatively charged groups and consequently, the uptake of the dye declined. According to Limei et al. [38] lower pH brought about a large number of H_3O^+ which caused a fierce competition in the ion-exchange sites inside the adsorbent but that as the pH increased, the protonated functional groups inside the adsorbent were deprotonated, thus, enhancing the adsorption capacity of the adsorbent material for adsorbate. Following the view of Kaushik et al. [39], an anionic dye that contained sulfonated organic azo compounds such as reactive yellow 145 dye in their structures produces sodium salts in aqueous solutions. In case of Cu(II) ions adsorption, information from the zero point charge (see Table 1) revealed that at low pH, the ESCCA surface is expected to be positively charged since at a pH greater than that of the zero point charge, the ESCCA surface is negatively charged and as such, there is a tough electrostatic attraction between the negatively charged surface of the adsorbent and the positively charged Cu^{2+} in the adsorbate solution which enhances the uptake of the metal ion at a higher

solution pH. Related developments had been documented in the sorption of reactive yellow 125 dye using natural phosphate [40], direct yellow 27 on poorly crystalline hydroxyapatite [41] and the sorption of copper on acid-activated groundnut husk [11]. The studies on pH values above 7 were not included because in alkaline pH, there is precipitation of Cu in the form of hydroxide.

Sorption kinetics

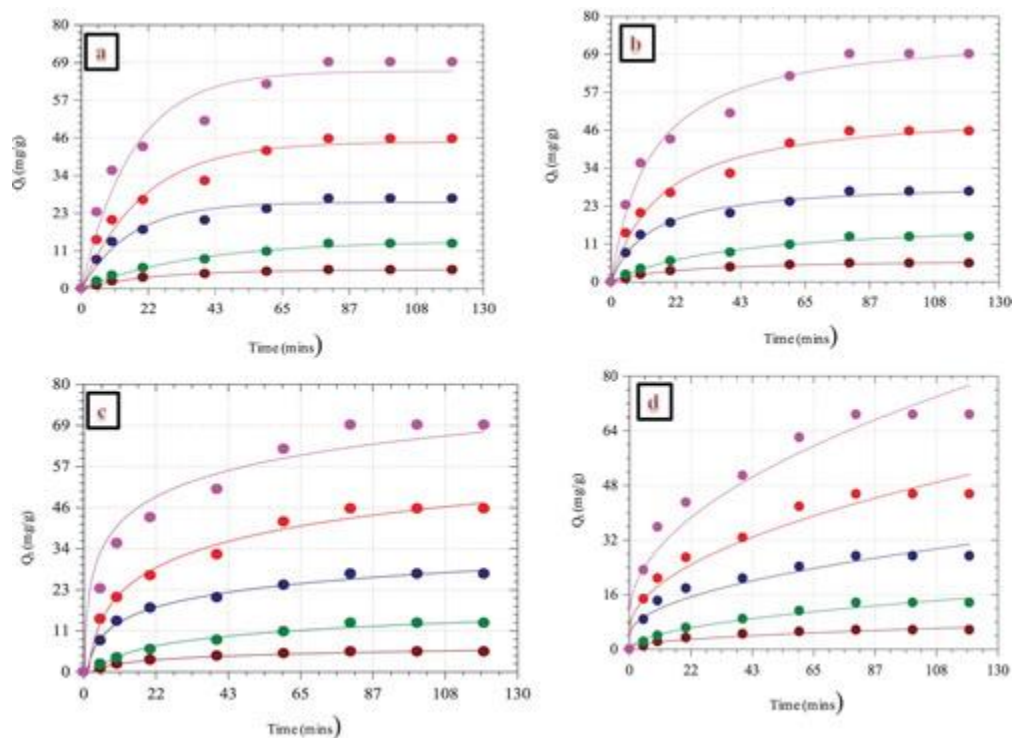
Kinetic investigation of adsorption data is a vital parameter in predicting the mechanism of the sorption process and also describes the sorption capability of ESCCA. Figures 7 and 8 were obtained from the kinetic models described in Equations (3)–(6), while the values of their constants are listed in Table 2 for Cu(II) and Table 3 for RY 145 dye, respectively. It was observed that the Pseudo-second-order kinetic model best described the adsorption of both Cu(II) ions and RY 145 dye. Though the correlation coefficient (R^2) values obtained from both Pseudo-first- and Pseudo-second-order kinetic models were high enough and close to unity, the second-order model was regarded as being the best fit owing to the closeness of the values of Q_e calculated, which were related to the Q_e experimental values. More also, %SSE values from Pseudo-second-order were smaller when compared with that of Pseudo-first-order kinetic model which implies that the uptake of Cu(II) ions and RY 145 dye onto the surface of the ESCCA adsorbent proceed via chemisorptions. The values of k_1 and k_2 obtained varied from 0.032 to 0.089 min^{-1} and from 1.078 to 2.722×10^3 mg/g/min for Cu(II) and from 0.027 to 0.063 min^{-1} and from 1.078–9.850 mg/g/min for RY 145 dye, respectively. Analysis of the Elovich model's parameter indicates an increase in the adsorption rate (α) with the pollutant concentration which could be due to an increase in the concentration gradient across the surface [5,11]. On the contrary, the values of the desorption rate (β) reduced as the concentration of pollutants increases which could be due to the formation of a chemical bond between the pollutant and functional groups present on the surface of ESCCA. This further confirmed that the adsorption process of Cu(II) ions and RY 145 dye onto the ESCCA surface is chemisorptions [41]. The intra-particle diffusion model was used to further evaluate the mechanisms of adsorption of Cu(II) and RY 145 dye onto the ESCCA surface and the physical parameters are reported in Table 2 for Cu(II) and Table 3 for RY 145 dye, respectively. The values of the intra-particle constants (K_{id}) increased with the concentration of the pollutants. According to Khalid et al. [41], the intra-particle diffusion may be regarded as 'concentration diffusion' when the values of the intraparticle constant increase with the increase in the pollutant concentration which corroborated the findings from this present study. In this study, the correlation coefficient (R^2) values are close to unity and it indicates that the intra-particle diffusion model describes the kinetic adsorption of Cu(II) and RY 145 dye onto ESCCA as well. The intra-particle diffusion model may be governed by surface diffusion or pore volume diffusion or through simultaneous processes [42]. Literature reports by Sharma et al. [43] and Guodong et al. [42] had it that adsorption proceeds via three steps with the first stage which is known as film diffusion involves the transport of the adsorbate from solution to the film surrounding of the adsorbent surface, the second stage known as pore or intra-particle diffusion which is the diffusion of the adsorbate from the film surface to the pore of the surface of the adsorbent and the last step is the adsorbate adsorption on the active adsorbing sites.

Figure 7. Kinetic fits for the adsorption of Cu(II) on ESCCA (a) pseudo-first-order model fits, (b) pseudo-second order model fits, (c) Elovich and (d) Intraparticle diffusion model fits. (Temperature: 35°C, pH: 5.0 and adsorbent dosage: 25 mg/L).



[Display full size](#)

Figure 8. Kinetic fits for the adsorption of RY 145 dye on ESCCA (a) pseudo-first-order model fits, (b) pseudo-second order model fits, (c) Elovich and (d) Intraparticle diffusion model fits. (Temperature: 35°C, pH: 5.0 and adsorbent dosage: 25 mg/L).



[Display full size](#)

Table 2. Kinetic values for the adsorption of Cu(II) ions by ESCCA.

[CSVDisplay Table](#)

Table 3. Kinetic parameters for the adsorption of RY 145 dye by ESCCA.

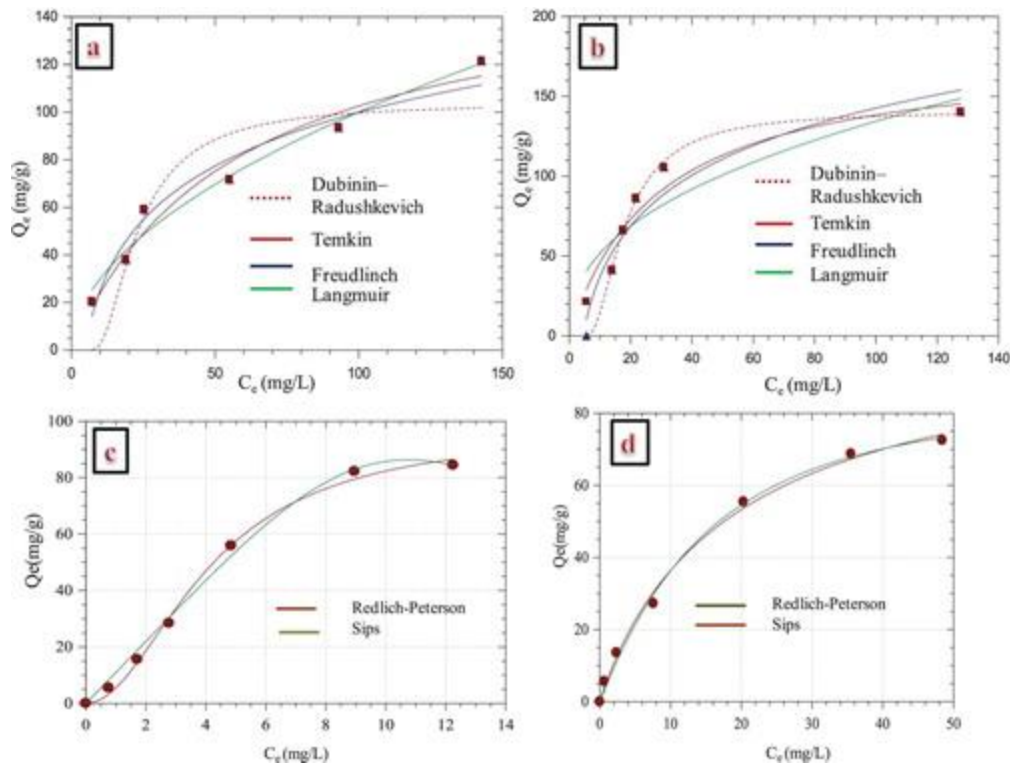
[CSVDisplay Table](#)

Adsorption isotherms

An adsorption isotherm is a vital tool in interpreting the distribution of solutes in aqueous solution and also to understand the adsorption capability of the adsorbent at equilibrium in order to maximise the use of adsorbents. [Figure 9\(a,b\)](#) depicts the plots of the two-parameter isotherms as described in Equations (8)–(11), while their physical parameters are listed in Table 4. In this present investigation, the range of pollutant's concentration used is 10–150 mg/L and it was observed that the correlation coefficient (R^2) value from Freundlich model is superior to the values of R^2 from other isotherms tested and as such, the adsorption process is well governed by Freundlich isotherm which assumes a mixed surface with interaction among adsorbed molecules (i.e chemisorptions) [44]. Since the values of n are higher than unity, the adsorption process is favourable [45]. The separation factor (R_L) from the Langmuir model was obtained from the expression: $R_L=1/(1+bC_0)$

(15) Values of R_L between 0 and 1 imply favourable adsorption, $R_L > 1$ indicates unfavourable adsorption, and $R_L = 0$ means irreversible process [45]. Thus, the values of $R_L < 1$ indicates a favourable adsorption process. The coefficient determination, $R^2 > 0.9$ for Cu(II), and RY 145 dye shows that the adsorption data of ESCCA is also described by the Temkin sorption isotherm. The utmost adsorption capacities derived from D-R isotherm are 65.17 and 49.62 mg/g for Cu(II) and RY 145 dye, respectively. The values of E obtained for Cu(II) and RY 145 are 10.87 and 12.85 kJ/mol, respectively and since these values are higher than 8 kJ/mol, the process of adsorption follows chemical adsorption [37,44]. For the three-parameter isotherms, their non-linear plots are represented in [Figure 9\(c,d\)](#), with their parameters listed in Table 4. The adsorption data matched well with both the Redlich–Peterson, and Sips isotherms which combine the features of Langmuir and Freundlich models. The values of the determination of coefficients (R^2) obtained are 0.998 and 0.986 for Redlich–Peterson model and 0.995 and 0.987 for the Sips model for the Cu(II) ions and reactive yellow 145 dye, respectively. On comparison, although the R^2 values from the two-parameters obtained were closed to unity, the three-parameters isotherms demonstrate higher values and base on this premises, the three-parameters isotherms were adjudged best fits for the adsorption of Cu(II) ions and RY 145 dye.

Figure 9. Isotherm plots of (a) and (b) two-parameters isotherm and (c) and (d) three-parameters isotherms fits for the adsorption of Cu(II) and RY145 dye by ESCCA (Initial pollutant concentration: 10–150 mg/L, Temperature: 35°C, pH: 2.0 and 5.0 and adsorbent dosage: 25 mg/L).



[Display full size](#)

Table 4. Isotherm Parameters for Cu(II) ions and RY145 dye Adsorption onto ESCCA.

[CSVDisplay Table](#)

Comparative study of adsorption capacity of ESCCA with previous works in literature

Comparative analysis of different adsorbents as obtained from literature reports with the as-prepared ESCCA, in the uptake of Cu(II) and RY 145 dye is presented in Table 5. It can be seen that the developed adsorbent enjoy high adsorption ability towards Cu(II) and RY 145 removal when contrasted with other literature adsorbents reported.

Table 5. Comparison of the adsorption capacities of ESCCA for Cu(II) and reactive 145 dye.

[CSVDisplay Table](#)

Study on the mechanism of pollutants adsorption by ESCCA

There exist various mechanisms such as surface sorption, ion exchange, precipitation, and electrostatic interaction for predicting the adsorption of pollutants by adsorbents [16]. Typical

adsorption mechanisms entailed the united effects of these different types of interactions which contain electrostatic attraction, van der Waals force, and chemical bond force [15,52]. First, the point of zero charge was used to describe the mechanism of the adsorption process since it's a measure of the electrostatic forces of interaction during the process of contaminants uptake which is a function of the solution pH [13]. From this present investigation, the value of the zero point charge indicated in Table 1 showed that the surface of the ESCCA is positively at lower pH and negatively charged at higher. Thus, the opposite charges between the pollutants and the ESCCA surface at different pH values resulted in electrostatic association which enhanced the uptake of the pollutants.

Furthermore, in adsorption process, when equilibrium is reach at constant temperature, the mechanism of the reaction can be explained in terms of the relationship between the adsorbent adsorption capacity, q_e , as well as the pollutant concentration at equilibrium and this can be mathematically described using certain isotherm models. In this present study, two and three parameters adsorption isotherm models were used to investigate the mechanism of the adsorption of Cu(II) and RY 145 dye by eggshell adsorbent. According to the data from the equilibrium adsorption capacity and on comparing the correlation coefficients of the two parameter models suggested that the adsorption process showed good fit to the Freundlich isotherm indicating that the adsorption of Cu(II) and RY 145 dye by ESCCA occurs via the mechanism predicted by chemisorptions. In the study conducted by Ajaelu et al. [51], it was concluded that the mechanism of adsorption of Cu (II) ions from aqueous solution by untreated *Tectona grandis* (UTG) and citric acid- modified *T. grandis* (CAMTG) bark powder were governed by the Freundlich.

Another important tool that is normally employed in explaining the mechanism of adsorption process is the application of various kinetic models which can be used to establish the rate-controlling step. The kinetics of Cu(II) and RY 145 dye adsorption process by ESCCA was elucidated by fitting the experimental data with Pseudo-first order, Pseudo-second order, Elovich and intraparticle diffusion kinetic models. It was discovered that the mechanism of Cu(II) and RY 145 dye was controlled by the Pseudo-second-order model because of the proper fitting of the experimental data (see Table 2), thus suggesting a chemisorption mechanism and also corroborated the results of the isotherm study [41]. Ajaelu et al. [51] reported that the Pseudo-second-order kinetic model has an outstanding suitability to the experimental data and thus best described the mechanism of copper (II) ion by *Tectona grandis* and citric acid- modified *T. grandis* bark powder. FT-IR analysis of the adsorbent before and after pollutants adsorption was equally deployed in other to further provide lucid explanation on the mechanism involved in the adsorption process of Cu(II) and RY 145cdye. From the FT-IR investigation, the major functional groups present on the surface of the adsorbent are hydroxyl and carbonyl which are negatively charged when deprotonated and can be electronically attached to Cu(II) ions at higher pH and to RY 145 dye which is anionic dye at lower pH. According to Xu et al. [53] negatively charged surface of the adsorbent can be attracted by the positively charged cations of organic structures like RY 145 dye at higher pH, while the electrostatic repulsion between the adsorbent and the negatively charged anions of the organic pollutants requires hydrogen bonding to be able to adhere strongly. Al-Senani et al. [50] observed that the rate limiting step in the adsorption of Cu(II) ions by two environment-friendly adsorbents prepared from *Origanum* (OR) and *Lavandula* (LV)) is chemisorption adsorption mechanism that involved valence forces via the exchange of electrons between the pollutant and the various functional groups present on the surface of the adsorbents. Yueming et

al. [4] using FT-IR to elucidate the adsorption mechanism of GNS/MnO₂ before and after Cu(II) adsorption and it was reported that the changes which occurred on the surface of the adsorbent after the uptake of the metal ion were due to the presence of hydroxyl groups on the adsorbent surface. They concluded that the mechanism involved in the uptake process of the pollutant is complexation reactions.

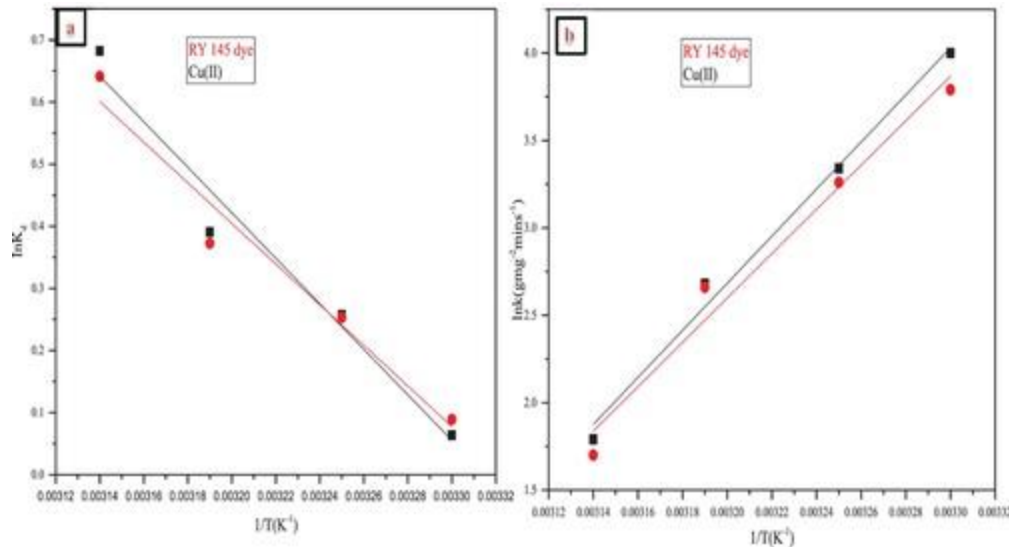
Thermodynamic analysis

The energy of activation (E_a) was evaluated by adopting the Arrhenius equation as represented in the relationship: $\ln k = \ln A - E_a/RT$

(16) where k (g/mg/min) is the Pseudo-second-order kinetic model rate constant, the activation energy of adsorption is denoted as E_a (kJ/mol), Arrhenius factor is designated as A , R is the universal gas constant (8.314 J/mol/K) and the absolute temperature is denoted as T in Kelvin. The change in free energy (ΔG°), change in enthalpy (ΔH°), and change in entropy (ΔS°) were computed as follows: $\Delta G^\circ = -RT \ln K_d$ (17) $\ln K_d = \Delta S^\circ/R - \Delta H^\circ/RT$

(18) The equilibrium constant, K_d , is obtained from the value of Q_e/C_e . The plots of $\ln K_d$ against $1/T$ should produce a straight line with slope and intercept of $\Delta H^\circ/R$ and $\Delta S^\circ/R$ respectively as shown in [Figure 10\(a\)](#), while the thermodynamic values evaluated are shown in Table 6. It was noticed that the K_d values rise with the temperature, which suggests the endothermic nature of the adsorption process. The positive value of ΔH (30452.020 and 27194.180 kJ/mol) for Cu(II) and RY 145 dye confirm the process of adsorption to be an endothermic reaction as well. The calculated values of ΔG were negative which increases with temperature, thus indicating the spontaneous nature of the adsorption process. The high value of ΔS (100.930 and 90.340 kJ/mol) for Cu(II) and reactive yellow 145 dye inferred high randomness of the adsorption process at the adsorbent–adsorbate interface. The plot of $\ln k$ against $1/T$ is shown in [Figure 10\(b\)](#) with linear relationship between the activation energy and the temperature. The activation energy (E_a) was found to be 34.46 and 28.22 kJ/mol for Cu(II) and RY 145 dye, respectively.

Figure 10. Thermodynamic plots for the adsorption of (a) Cu(II) and (b) RY145 dye by ESCCA (Initial pollutant concentration: 10–150 mg/L, Temperature: 35°C, pH: 2.0 and 5.0 and adsorbent dosage: 25 mg/L).



[Display full size](#)

Table 6. Thermodynamic parameters for the adsorption of Cu(II) and reactive 145 dye by ESCCA powder.

[CSVDisplay Table](#)

Conclusions

Cumulative findings are summarised as follows:

1. XRD revealed that the adsorbent is made up of a Rhombohedral non-crystalline structure. TEM and SEM analyses both suggest round particle morphology, while FT-IR confirmed the existence of calcite functional groups.
2. The amount of copper (II) ions and RY 145 dye eliminated from the aqueous solution increase with the contact time, adsorbate concentrations, and the adsorbent dosage, while maximum uptake of Cu(II) ion and RY 145 dye was attained at solution pH of 5.0 and 2.0, respectively.
3. The adsorbent showed better adsorption affinity towards Cu(II) ions compared with the dye.
4. The kinetic analysis reveals that the uptake of both adsorbates follow Pseudo-second-order kinetic model thus suggesting a chemisorptions process and this was corroborated from adsorption isotherm analysis which matched well with the isotherm of Freundlich.
5. Thermodynamic parameters suggest that the process of adsorption was endothermic, feasible, and spontaneous.

Thus, the applicability of low-cost adsorbent obtained from agro-waste of eggshell for wastewater treatment is feasible.

Acknowledgements

The authors are grateful for the financial supports received by Ofudje A. Edwin from the Department of Science and Technology (DST), Government of India. The authors also express their profound gratitude to the Technical staff of Central Instrumentation Facility, CSIR-CECRI, Tamil Nadu, India, for their support in FT-IR, TEM, SEM, and XRD analyses.

Disclosure statement

No potential conflict of interest was reported by the author(s).

Notes on contributor

Dr. Edwin A. Ofudje is a Senior Lecturer at the Department of Chemical Sciences, College of Basic and Applied Sciences, Mountain Top University, Ogun State, Nigeria. He is the Ag. Director of the Centre for Research, Innovation and Collaborations, Mountain Top University, Nigeria and his area of specialization includes Physical/Environmental/Material Chemistry.

Dr. Ezekiel F. Sodiya is a Lecturer at the Department of Chemical Sciences, College of Basic and Applied Sciences, Mountain Top University, Ogun State, Nigeria. He is interested in corrosion and environmental pollution research.

Dr. Francis H. Ibadin is a Lecturer at the Department of Biological Sciences, College of Basic and Applied Sciences, Mountain Top University, Ogun State, Nigeria. His research focus is on environmental biology and toxicology.

Mrs. Abimbola A. Ogundiran is a Lecturer at the Department of Chemical Sciences, Tai Solarin University of Education, Ijebu-Ode, Ogun State. She is a Ph.D student at the Department of Chemistry, Olabisi Onanbajo University, Nigeria. She is focused on Physical Chemistry and pollution research.

Dr. Samson O. Alayande is currently working as a Senior Lecturer, Department of Physical Science, First Technical University (Tech-U), Ibadan, Nigeria. He is the Ag. Director, Intellectual Property and Technology Transfer Office, First Technical University (Tech-U), Ibadan, Nigeria. He has excellent research contributions in the Industrial Chemistry, Environmental and Material Science.

Dr. (Mrs) Oluremi A. Osideko was awarded a Ph.D in Physical Chemistry from Federal University of Agriculture Abeokuta, Ogun State Nigeria. Dr. Osideko is interested in the research area of Physical and Environmental Chemistry.

Additional information

Funding

This work was financially supported by Ofudje A. Edwin from the Department of Science and Technology (DST), Government of India.

References

- GuptaA, RaiDK, PandeyRS, et al. Analysis of some heavy metals in the riverine water, sediments and fish from river Ganges at Allahabad. *Environ Monit Assess.* 2009;157:449–458. [[Crossref](#)], [[PubMed](#)], [[Web of Science ®](#)], [[Google Scholar](#)]
- AgahH, LeermakersM, ElskensM, et al. Accumulation of trace metals in the muscles and liver of five fish species from the Persian Gulf. *Environ Monit Assess.* 2009;157:499–514. [[Crossref](#)], [[PubMed](#)], [[Web of Science ®](#)], [[Google Scholar](#)]
- LinnikPM, ZubenkoIB. Role of bottom sediments in the secondary pollution of aquatic environments by heavy metal compounds. *Lakes Reserv Res Manage.* 2000;5:11–21. [[Crossref](#)], [[Google Scholar](#)]
- YuemingR, NiY, JingF, et al. Adsorption mechanism of copper and lead ions onto graphene nanosheet/ δ -MnO₂. *Mater Chem Phys.* 2012;136:538e–5544. [[Crossref](#)], [[Web of Science ®](#)], [[Google Scholar](#)]
- AdeogunAI, OfudjeEA, IdowuMA, et al. Biosorption of Cd²⁺ and Zn²⁺ from aqueous solution using tilapia fish scale (*Oreochromis* sp): kinetics, isothermal and thermodynamic study. *Desalin Water Treat.* 2018;107:182–194. [[Crossref](#)], [[Web of Science ®](#)], [[Google Scholar](#)]
- HughesMN. *The inorganic chemistry of biological process.* London: Willey interscience pub; 1975. [[Google Scholar](#)]
- TirkeyA, ShrivastavaP, SaxenaA. Bioaccumulation of heavy metals in different components of two Lakes ecosystem. *Curr World Environ.* 2012;7:293–297. [[Crossref](#)], [[Google Scholar](#)]
- PolyaMM, VarbinaRL. Investigations on the dyeing ability of some reactive triazine azo ayes containing tetramethylpiperidine fragment. *J Chem Technol Metall.* 2017;52:3–12. [[Google Scholar](#)]
- LodhaB, ChaudhariS. Optimization of Fenton-biological treatment scheme for the treatment of aqueous dye solutions. *J Hazard Mater.* 2007;148:459–466. [[Crossref](#)], [[PubMed](#)], [[Web of Science ®](#)], [[Google Scholar](#)]
- SleimanM, VildozaD, FerronatoC, et al. Photocatalytic degradation of azo dye Metanil yellow: optimization and kinetic modeling using a chemometric approach. *Appl Catal B: Environ.* 2007;77:1–11. [[Crossref](#)], [[Web of Science ®](#)], [[Google Scholar](#)]
- OfudjeEA, AwotulaAO, HambateGV, et al. Acid activation of groundnut husk for copper adsorption: kinetics and equilibrium studies. *Desalin Water Treat.* 2017;86:240–251. [[Crossref](#)], [[Web of Science ®](#)], [[Google Scholar](#)]
- AliI, GuptaV. Advances in water treatment by adsorption technology. *Nat Protoc.* 2006;1:2661–2667. [[Crossref](#)], [[PubMed](#)], [[Web of Science ®](#)], [[Google Scholar](#)]
- ZohaibA, ShafaqatA, MuhammadR, et al. A critical review of mechanisms involved in the adsorption of organic and inorganic contaminants through biochar. *Arabian J Geosci.* 2018;11:448. doi:10.1007/s12517-018-3790-1. [[Crossref](#)], [[Web of Science ®](#)], [[Google Scholar](#)]
- ChenT, YingL, JingW, et al. Characterization and mechanism of copper biosorption by a highly copper resistant fungal strain isolated from copper-polluted acidic orchard soil.

Environ Sci Pollut Res Int. 2018;25:24965–24974. doi:10.1007/s11356-018-2563-4. [[Crossref](#)], [[PubMed](#)], [[Web of Science ®](#)], [[Google Scholar](#)]

- LiangC, HongYH, WanTZ, et al. Adsorption mechanism of copper ions in aqueous solution by chitosan–carboxymethyl starch composites. J Appl Polym Sci. 2019. doi:10.1002/APP.48636. [[Crossref](#)], [[Web of Science ®](#)], [[Google Scholar](#)]
- YounisU, MalikSA, RizwanM, et al. Biochar enhances the cadmium tolerance in spinach (*Spinacia oleracea*) through modification of Cd uptake and physiological and biochemical attributes. Environ Sci Pollut Res. 2016;23:21385–21394. [[Crossref](#)], [[PubMed](#)], [[Web of Science ®](#)], [[Google Scholar](#)]
- CalimanLB, da SilvaSN, JunkesJA, et al. Ostrich eggshell as an alternative source of calcium ions for biomaterials synthesis. Mater Resear. 2017;20:413–417. [[Crossref](#)], [[Web of Science ®](#)], [[Google Scholar](#)]
- OfudjeEA, AkiodeOK, OladipoGO. Application of alkaline-modified coconut shaft as a biosorbent for Pb²⁺ removal. Bioresource. 2015;10:3462–3480. [[Crossref](#)], [[Web of Science ®](#)], [[Google Scholar](#)]
- OfudjeEA, AkinbileB, AwotulaAO, et al. Kinetic studies of thiocyanate ions removal from aqueous solution using carbonaceous Guinea-corn. J Sci Resear. 2015;14:94–101. [[Google Scholar](#)]
- HoYS, MckayGM. Sorption of copper (II) from aqueous solution by peat. water. Air Soil Poll. 2004;158:77–97. [[Crossref](#)], [[Web of Science ®](#)], [[Google Scholar](#)]
- WeberWJ, MorrisJC. Kinetic of adsorption on carbon from solution. J Sanit Eng Div Proc Amer Soci Civil Eng. 1963;89:31–60. [[Google Scholar](#)]
- CheungCW, PorterJF, McKayG. Sorption kinetic analysis for the removal of cadmium ions from effluents using bone char. Water Res. 2001;35:605–612. [[Crossref](#)], [[PubMed](#)], [[Web of Science ®](#)], [[Google Scholar](#)]
- AdeogunAI, OfudjeEA, IdowuMA, et al. Kinetic, thermodynamic and isotherm parameters of biosorption of Cr(VI) and Pb (II) ions from aqueous solution by Biosorbent prepared from Corncob biomass. Ind J Inorg Chem. 2012;7:119–129. [[Google Scholar](#)]
- FreundlichHMF. Über die adsorption in lösungen. Z Phys Chem. 1960;57:385–470. [[Google Scholar](#)]
- LangmuirI. The adsorption of gases on plane surfaces of glass, mica and platinum. J Am Chem Soc. 1918;40:1361–1403. [[Crossref](#)], [[Web of Science ®](#)], [[Google Scholar](#)]
- TemkinMJ, PyzhevV. Recent modifications to Langmuir isotherms. Acta Physiochim USSR. 1940;12:217–222. [[Google Scholar](#)]
- DubininMM, ZaverinaED, RadushkevichLV. Sorption and structure of active carbons. I Adsorption of organic vapors. Zh Fiz Khim. 1947;21:1351–1362. [[Google Scholar](#)]
- SipsR. Combined form of Langmuir and Freundlich equations. J Chem Phys. 1948;16:490–495. [[Crossref](#)], [[Web of Science ®](#)], [[Google Scholar](#)]
- RedlichO, PetersonDL. A useful adsorption isotherm. J Phys Chem. 1959;63:1024. [[Crossref](#)], [[Web of Science ®](#)], [[Google Scholar](#)]
- OfudjeEA, WilliamsOD, AsogwaKK, et al. Assessment of Langmuir, Freundlich and Rubunin - Radushhkevich adsorption isotherms in the study of the biosorption of Mn (II) ions from aqueous solution by untreated and acid-treated corn shaft. Int J Sci Eng Res. 2013;4:1628–1634. [[Google Scholar](#)]

- MeriemB, FatimaA. Comparative adsorption isotherms and modeling of methylene blue onto activated carbons. *Appl Water Sci.* 2011;1:111–117. doi:10.1007/s13201-011-0014-1. [[Crossref](#)], [[Google Scholar](#)]
- WangC, XiaoP, ZhaoJ, et al. Biomimetic synthesis of hydrophobic calcium carbonate nanoparticles via a carbonation route. *Powder Technol.* 2006;170:31. [[Crossref](#)], [[Web of Science ®](#)], [[Google Scholar](#)]
- AdeogunAI, OfudjeEA, IdowuMA, et al. Facile Development of Nano Size Calcium Hydroxyapatite based ceramic from eggshells: synthesis and characterization. *Waste Biomass Valor.* 2017;4; doi:10.1007/s12649-017-9891-3. [[Crossref](#)], [[Google Scholar](#)]
- BartczakP, NormanM, KlapiszewskiL, et al. Removal of nickel(II) and lead(II) ions from aqueous solution using peat as a low-cost adsorbent: a kinetic and equilibrium study. *Arabian J Chem.* 2015. doi:10.1016/j.arabjc.2015.07.018. [[Crossref](#)], [[Google Scholar](#)]
- KumarPGVSR, MallaKA, YerraB, et al. Removal of Cu(II) using three low-cost adsorbents and prediction of adsorption using artificial neural networks. *Appl Water Sci.* 2019;9:44. doi:10.1007/s13201-019-0924-x. [[Crossref](#)], [[Web of Science ®](#)], [[Google Scholar](#)]
- LiQ, ZhaiJ, ZhangW, et al. Kinetic studies of adsorption of Pb(II), Cr(III) and Cu(II) from aqueous solution by sawdust and modified peanut husk. *J Hazard Mater B.* 2006;141:163–167. [[Crossref](#)], [[PubMed](#)], [[Web of Science ®](#)], [[Google Scholar](#)]
- AdeogunAI, OfudjeEA, IdowuMA, et al. Equilibrium, kinetic and thermodynamic studies of the biosorption of Mn (II) ions from aqueous solute and acid-treated corncob. *Bioresources.* 2011;6:4117–4134. [[Web of Science ®](#)], [[Google Scholar](#)]
- LimeiC, YaoguangW, LihuaH, et al. Mechanism of Pb(II) and methylene blue adsorption onto magnetic carbonate hydroxyapatite/grapheme oxide. *RSC Adv.* 2015;5:9759. [[Crossref](#)], [[Web of Science ®](#)], [[Google Scholar](#)]
- KaushikCP, TutejaR, KaushikN, et al. Minimization of organic chemical load in direct dyes effluent using low cost adsorbents. *Chem Eng J.* 2009;155:234–240. [[Crossref](#)], [[Web of Science ®](#)], [[Google Scholar](#)]
- BarkaN, AssabbaneA, NounahA, et al. Removal of textile dyes from aqueous solutions by natural phosphate as a new adsorbent. *Desalination.* 2009;235:264–275. [[Crossref](#)], [[Web of Science ®](#)], [[Google Scholar](#)]
- MahmudK, Azharull, AnastasiosM, et al. Adsorption of direct yellow 27 from water by poorly crystalline hydroxyapatite prepared via precipitation method. *Desalin Water Treat.* 2012;41:170–178. [[Taylor & Francis Online](#)], [[Web of Science ®](#)], [[Google Scholar](#)]
- GuodongS, YiminL, XinY, et al. Efficient removal of arsenate by versatile magnetic graphene oxide composites. *RSC Adv.* 2012;2:12400–12407. [[Crossref](#)], [[Web of Science ®](#)], [[Google Scholar](#)]
- SharmaYC, SrivastavaV, MukherjeeAK. Synthesis and application of nanoAl₂O₃ powder for the reclamation of hexavalent chromium from aqueous solutions. *J Chem Eng Data.* 2010;55:2390–2398. [[Crossref](#)], [[Web of Science ®](#)], [[Google Scholar](#)]
- OfudjeEA, AdeogunAI, IdowuMA, et al. Simultaneous removals of cadmium (II) ions and reactive yellow 4 dye from aqueous solution by bone meal derived apatite: kinetics, equilibrium and thermodynamic evaluations. *J Anal Sci Technol.* 2020;11:7. doi:10.1186/s40543-020-0206-0. [[Crossref](#)], [[Web of Science ®](#)], [[Google Scholar](#)]

- XuD, TanXL, ChenCL, et al. Adsorption of Pb(II) from aqueous solution to MX-80 bentonite: effect of pH, ionic strength, foreign ions and temperature. *Appl Clay Sci.* 2008;41:37–46. [\[Crossref\]](#), [\[Web of Science ®\]](#), [\[Google Scholar\]](#)
- RatanaS, WipharatCC, KanokwanW. Adsorption of reactive dyes Red 195, Blue 222, and yellow 145 in solution with Polyaniline-chitosan membrane using batch Reactor. *Key Eng Mater.* 2017;751:713–718. doi:10.4028/www.scientific.net/KEM.751.713. [\[Crossref\]](#), [\[Google Scholar\]](#)
- EmmanJM, AbbasJL, SalihHK. Photocatalytic removal of reactive yellow 145 dye from simulated textile wastewaters over supported (Co, Ni)₃O₄/Al₂O₃ co-catalyst. *Polish J Chem Technol.* 2016;18:1–9. [\[Crossref\]](#), [\[Web of Science ®\]](#), [\[Google Scholar\]](#)
- AbbasJL. Effect of activation temperature on ability of activated carbon on removal of reactive yellow 145 dye from simulated industrial textile wastewaters. *J Chem Pharm Res.* 2015;7:158–169. [\[Google Scholar\]](#)
- KrishnaniKK, MengX, ChristodoulatosC, et al. Biosorption mechanism of nine different heavy metals onto biomatrix from rice husk. *J Hazard Mater.* 2008;153:1222–1234. [\[Crossref\]](#), [\[PubMed\]](#), [\[Web of Science ®\]](#), [\[Google Scholar\]](#)
- Al-SenaniG, Al-FawzanFF. Study on adsorption of Cu and Ba from aqueous solutions using nanoparticles of Origanum (OR) and Lavandula (LV). *Bioinorg Chem Appl.* 2018. doi:10.1155/2018/3936178. [\[Crossref\]](#), [\[PubMed\]](#), [\[Web of Science ®\]](#), [\[Google Scholar\]](#)
- AjaeluCJ, IbironkeL, OladinniAB. Copper (II) ions adsorption by untreated and chemically modified *Tectona grandis* (Teak bark): kinetics, equilibrium and thermodynamic studies. *Afr J Biotechnol.* 2019;18:296–306. doi:10.5897/AJB2018.16740. [\[Crossref\]](#), [\[Google Scholar\]](#)
- PatraJM, PandaSS, DhalNK. Biochar as a low-cost adsorbent for heavy metal removal: a review. *Int J Res Biosci.* 2017;6:1–7. [\[Google Scholar\]](#)
- XuXY, SchierzA, XuN, et al. Comparison of the characteristics and mechanisms of Hg(II) sorption by biochars and activated carbon. *J Colloid Interf Sci.* 2016;463:55–60. [\[Crossref\]](#), [\[PubMed\]](#), [\[Web of Science ®\]](#), [\[Google Scholar\]](#)